

Experimental Study of Enhanced Melting Process Under Ultrasonic Influence

K. J. Choi* and J. S. Hong†

University of Illinois at Chicago, Chicago, Illinois 60680

The effects of ultrasonic vibrations on the melting process of phase change material (PCM) in a rectangular vessel were experimentally investigated. A constant heat flux from a vertical heating plate was provided to the PCM. Ultrasonic vibrations were applied through a bottom plate of the enclosure. Three different heat fluxes and various ultrasonic frequencies in the range of 15 to 55 KHz were tested. The heat transfer coefficients on the heating plate, the solid-liquid interface shape, and the temperature distributions in the PCM during a complete melting process were measured at various experimental conditions. The results show that the overall melting phenomena was significantly affected by the ultrasonic vibrations and the change in frequency of the ultrasonic waves.

Nomenclature

c_p	= specific heat
f	= frequency of ultrasonic vibrations
$ Fo$	= Fourier number, $\alpha t/H^2$
$ Fo_f$	= Fourier number at the end of melting process
g	= gravitational acceleration
h	= heat transfer coefficient
Δh_f	= latent heat of fusion
H	= initial PCM height
k	= thermal conductivity of PCM
L	= initial PCM length
Nu	= Nusselt number on the heater surface, hH/k
Pr	= Prandtl number of PCM, ν/α
q	= heat power
q''	= heat flux
Ra	= Rayleigh number, $g\beta\Delta T H^3/\nu\alpha$
Ra^*	= modified Rayleigh number, $g\beta q'' H^4/\nu\alpha k$
s	= location of melting front
Ste	= Stefan number, $c_p\Delta T/\Delta h_f$
Ste^*	= modified Stefan number, $c_p q'' H/k \Delta h_f$
t	= time
T	= temperature
W	= initial PCM width
x, y, z	= cartesian coordinates; see Fig. 1
X, Y, Z	= dimensionless coordinates, $x/L, y/H, z/W$
α	= thermal diffusivity
β	= thermal expansion coefficient
Γ	= dimensionless location of melting front, s/H
η	= melting efficiency
θ	= dimensionless temperature of PCM, $k(T - T_f)/q''H$
ν	= kinematic viscosity of PCM
ρ	= density of PCM

Subscripts

f	= at fusion condition
w	= at heater surface

Introduction

MELTING phenomena of phase change material (PCM) is of great importance in diverse engineering applica-

tions, such as metallurgy, thawing of frozen soil, purification of materials, and latent heat of fusion energy systems. Due to such a wide range of applications, the phase change heat transfer of melting has received considerable attention,¹⁻⁴ and a comprehensive review of the studies is reported in the literature.⁵

In the melting process of PCM, natural convective flow in the molten liquid usually plays an important role for the enhancement in melting. Many studies have dealt with the natural convective flows during the melting process.⁶⁻⁸ However, at certain extreme conditions, such as in space, the natural convection does not play a significant role in the melting process, due to the weak gravitational field. In such a case, the melting process will be greatly retarded. For application of the phase-change heat transfer to the future space power systems,⁹ such aggravated heat transfer problems should be solved. The present study is aimed at exploring a potential technique for the use of ultrasonic vibrations as a remedy for the expected phase-change heat transfer problems.

In the past, most use of ultrasonic vibrations was related to certain chemical processes¹⁰ and the medical industry. Only limited cases of study were concerned with heat transfer problems.¹¹⁻¹⁵ Lemlich¹¹ studied the effect of vibrations on natural convective heat transfer from a heated wire to air. Larson and London¹² studied the ultrasonic effect on both natural and forced convection heat transfer. They reported that a significant increase in heat transfer was observed for the natural convective heat transfer, whereas it was negligible for the forced convection case at high Reynolds numbers. Raben¹³ also reported that the enhancement by acoustic vibrations in the forced convection heat transfer was observed at only low Reynolds numbers. Wong and Chon¹⁴ and Park and Bergles¹⁵ investigated the effects of ultrasonic vibrations on the boiling heat transfer, including burnout heat flux. Their studies revealed no significant effect of ultrasonic vibrations on the boiling heat transfer.

No studies of ultrasonic effect on the melting phenomena, except Fairbanks' work,¹⁶ were conducted. In his study, the influence of ultrasound on melting of frozen coal slurry was investigated, and a significant influence of the ultrasound was reported. However, his research method is considered as preliminary, and the results were not generalized well. For better understanding of the ultrasonic influence on the overall melting phenomena, systematic experiments are required. In this paper, the authors report the ultrasonic effects on the melting process of a petroleum-derived hydrocarbon (99% pure n-octadecane). The heat transfer rate from the vertical heater surface to the PCM, the solid-liquid interface shape, and the

Received Jan. 4, 1990; revision received June 4, 1990; accepted for publication June 5, 1990. Copyright © 1990 by the American Institute of Aeronautics and Astronautics, Inc. All rights reserved.

*Assistant Professor, Mechanical Engineering Department. Member AIAA.

†Graduate Student, Mechanical Engineering Department.

PCM temperature variations with time in three dimensions were measured at various ultrasonic frequencies in the range of 15–55 KHz. A comparison of melting phenomena was also made between the ultrasonic application and the nonapplication cases.

Analysis of Experimental Results

The analytical approach of the melting phenomena in a finite enclosure is complicated because a nonsteady state multidimensional process, as well as an irregular moving boundary problem, are involved. Furthermore, when ultrasonic vibrations are applied to the melting process, the problem becomes much more complicated. Therefore, in order to find valuable experimental parameters, a simpler two-dimensional model without ultrasonic application, which Ho and Viskanta⁷ have developed, was employed in this study. The geometrical configuration used in the analysis is shown in Fig. 1. Both the top and bottom surfaces of the enclosure are assumed to be insulated. Based on the two-dimensional model, along with some assumptions, the nonsteady governing equations of vorticity and energy are expressed in terms of dimensionless variables, such as X , Y , Fo , Pr , and Ra . The initial condition and the boundary conditions on both the solid-liquid interface and the heater surface are also expressed in terms of the above dimensionless variables, as well as the Stefan Number Ste . However, in this study a constant heat flux from the heating surface was assumed during a complete melting process, so a modified Stefan Number Ste^* , a modified Rayleigh number Ra^* , and a dimensionless temperature θ were used. Furthermore, since a single value of Pr was tested, the effect of the Prandtl number was not investigated in this study. The experimental results, such as the heat transfer coefficient at the heater surface, the solid-liquid interface motion, and the dimensionless temperature in the PCM were presented in terms of X , Y , Fo , Ra^* , and Ste^* as follows, respectively:

$$Nu = f_1(Fo, Ste^*, Ra^*) \quad (1)$$

$$\Gamma = f_2(X, Y, Fo, Ste^*, Ra^*) \quad (2)$$

and

$$\theta = f_3(X, Y, Fo, Ste^*, Ra^*) \quad (3)$$

where f_1 , f_2 , and f_3 are certain functions. All these results are independently obtained at different ultrasonic frequencies and compared with those for the natural melting case.

Experimental Apparatus and Procedure

The overall schematic of the experimental apparatus is shown in Fig. 2. The experimental apparatus consists of three major

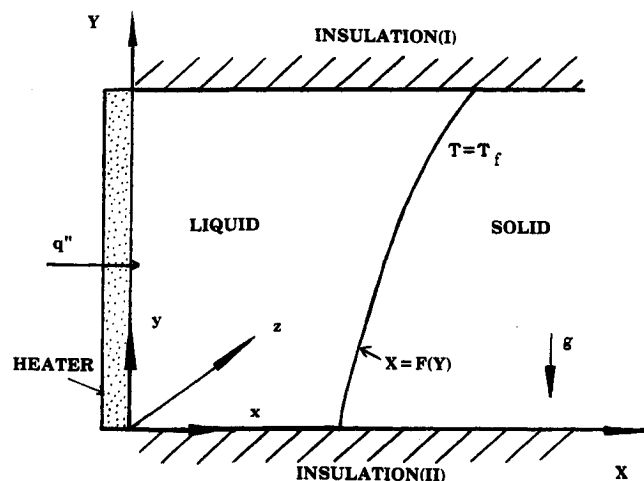


Fig. 1 Geometric configuration of the problem.

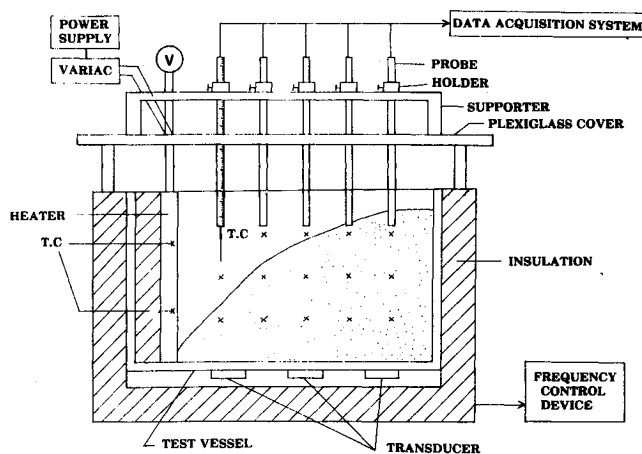


Fig. 2 Schematic of test setup.

parts, namely, an ultrasonic tank, a power supply unit, and an ultrasound control unit. The geometrical configuration of the rectangular vessel is described in detail in the literature,⁴ therefore, only a brief summary will be given. The inner dimensions of the tank were 16.5 cm high, 23.7 cm long, and 15.2 cm wide. One vertical wall of the ultrasonic tank is a heating plate generating a constant heat flux. The heating plate was made of two separated copper plates. A 1.5 mm diameter nickel-chromium wire was imbedded in the serpentine grooves between the two copper plates so that electric power could be evenly distributed over the heating plate. The outside surface of the heating plate was well insulated with thick fiberglass insulation material, while the inner surface made contact with the PCM. The bottom surface of the vessel was vibrated at ultrasonic frequency. For this purpose, three piezo-electric transducers of 3.5 cm diameter were placed on the outside surface of the bottom plate. The total energy input to the three transducers was about 60 W. In order to control the frequency of the vibrations in the range of 15–55 KHz, a frequency control circuit was built at the Electrical Engineering laboratory at the University of Illinois at Chicago.

In order to observe the solid-liquid interface, nine aluminum probes, on which fine scales were marked, were used at nine different preselected positions along the side and centerline, as shown in Fig. 2. For the temperature measurement during the melting process, a total of twenty-nine chromel-alumel (k-type) thermocouples of 0.5 mm diameter were installed at preselected locations in both the heating plate and the PCM. All but two thermocouples were placed in the PCM to measure the transient three-dimensional temperatures. Nine different locations on the horizontal plane (x - z plane) and three of each on the vertical plane (x - y plane) were selected. The two other thermocouples were embedded in the copper heating plate through small holes drilled from the back of the plate. The thermocouples were positioned in an array along the vertical center line at 6.1 cm and 12.1 cm from the bottom of the enclosure, respectively. The tip of the thermocouples was set 1.5 mm from the inner surface of the heating plate. Two different experiments were conducted independently: temperature measurement and solid-liquid interface shape measurement. The thermocouples and the aluminum probes were supported by an aluminum plate holder that regulates the probe height, secures the probes in place, and correctly locates the thermocouples. In order to investigate the agitation effect of ultrasonic vibrations on the enhancement in the melting process, a small mechanical stirrer of 3.0 cm diameter was used. The stirrer, held with a firm stand, was electrically operated. Due to the nature of these experiments, the actual experiment was carried out in a partially uninsulated container, i.e., the upper portion of the PCM in the container was in contact with the room air of 23°C.

Table 1 Thermophysical properties of n-octadecane

Properties	Measurements
Thermal conductivity (k)	0.24 W/m C
Density (ρ)	850 Kg/m ³
Latent heat (h_f)	241.3 KJ/Kg
Specific heat (C_p)	2.89 KJ/Kg C
Fusion temperature (T_f)	53.2 C
Kinematic viscosity (ν) at 50 C	4.0×10^{-6} m ² /s
Thermal expansion coefficient (β)	1.0×10^{-3} C ⁻¹

Table 2 Summary of experimental conditions

	q_w , W	q_w'' , W/m ²	H , m	f , KHz
Without ultrasound	118	5.1×10^3	0.152	0
	190	8.2×10^3	0.152	0
	252	10.9×10^3	0.152	0
With ultrasound	118	5.1×10^3	0.152	50
	190	8.2×10^3	0.152	50
	252	10.9×10^3	0.152	15–55

A petroleum-derived hydrocarbon (99% pure n-octadecane) was selected as the PCM, since it is a reasonably well-established, stable, and desirable material for melting experiments. The average thermophysical properties of the PCM are summarized in Table 1. Liquid paraffin was first filled in the ultrasonic tank. After complete solidification, slight irregularities and cavities on the top surface of the PCM were eliminated by refilling liquid PCM. The added volume of liquid was measured, and then, later, the same amount of PCM was taken out from the tank before resolidification for the next experiment. The dimensions of solid PCM used in this study were 15.2 cm high, 23.7 cm long, and 15.2 cm wide. The uniform initial temperature of the PCM was obtained after allowing it one day to reach equilibrium. After the desired conditions were established, a preselected heat flux was applied to the PCM. Also, a constant ultrasonic frequency, one of five (15, 25, 35, 50, and 55 KHz), was applied. The different experimental conditions used in this study are summarized in Table 2. For the mechanical stirring tests, the stirrer was operated in the melted PCM. For this purpose, the PCM was first heated at certain heat power and then the stirrer was applied to agitate the molten PCM. Two different experiments were conducted, i.e., the stirring was applied at 30 and 90 min, respectively, after the heater was turned on. Under the agitating condition, the heat transfer rate from the heating plate and the melting time was measured.

Results and Discussion

Heat Transfer from Heater Surface

The average heater temperature was calculated by arithmetically averaging the two local heater temperatures, which were usually within 2 K difference. Figure 3 is a typical average heater temperature variation with an actual time during a complete melting process at a heat flux of 8.21×10^3 W/m² (total heat power of 160 W) and an ultrasonic frequency of 50 KHz. The results of five individual tests conducted under the same experimental conditions show good repeatability. From these results, it is obvious that at an early stage of the melting process, the conduction mode is dominant in PCM. However, as time passes, natural convection becomes dominant, resulting in a decrease of the heater temperature. The fluctuation in the heater temperature due to the ultrasonic vibrations is also observed during the time period when natural convection is dominant.

The heater surface temperature and the fusion temperature of PCM ($T_f = 53.3^\circ\text{C}$) were used to calculate the heat transfer coefficient, or Nusselt number, on the heater surface. The variations of the dimensionless heat transfer parameter

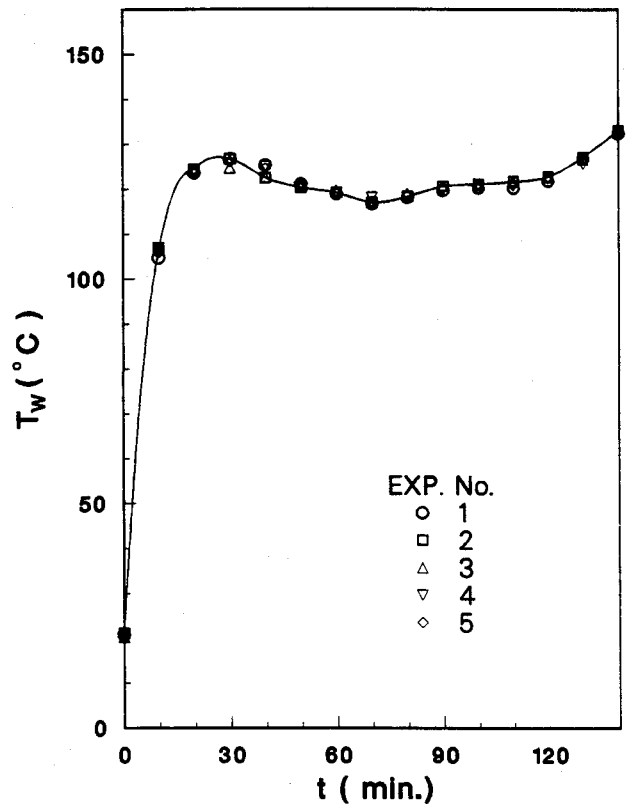


Fig. 3 Heater temperature distribution with time, $Ra^* = 0.77 \times 10^9$.

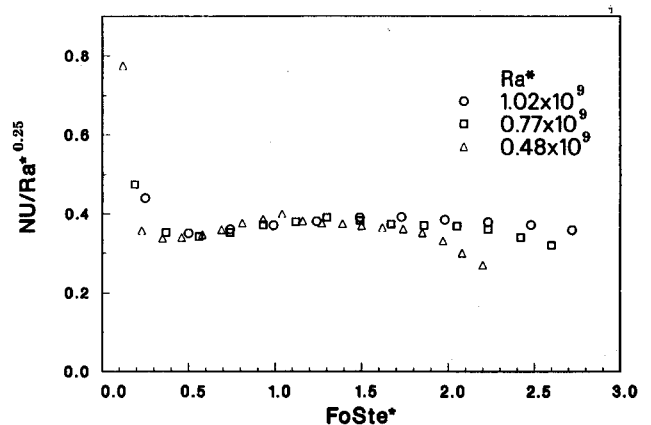


Fig. 4 Dimensionless heat transfer variations on heater surface with dimensionless time under ultrasonic influence ($f = 50$ KHz).

$Nu/Ra^{1/4}$ with dimensionless time $Fo \cdot Ste^*$ at three different heat fluxes are plotted in Fig. 4. As reported in the literature,¹ the parameter $Nu/Ra^{1/4}$ shows large deviations at early times because the melted layer is relatively thin, and, therefore, heat transfer is dominated by conduction. Unlike the natural melting case,⁴ the heat transfer behavior on the heater surface cannot be generalized by using these dimensionless parameters. This is due to the effects of ultrasonic vibrations on the melting phenomena.

A comparison of the heat transfer on the heater surface with ultrasonic vibrations at 50 KHz and without ultrasonic vibrations is given in Fig. 5. Both experiments were conducted under the same experimental conditions. As shown in the figure, the onset of dominant natural convection for both cases takes place at the same time, i.e., $Fo \cdot Ste^* = 0.6$, but the total melting times are apparently different. The heat transfer coefficients for the natural melting case are higher than those for melting with ultrasonic vibrations in the early stage of

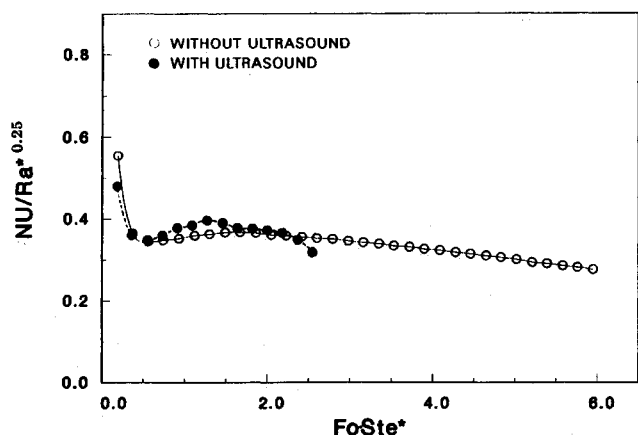


Fig. 5 Comparison of heat transfer coefficients with and without ultrasonic application, $Ra^* = 0.77 \times 10^9$.

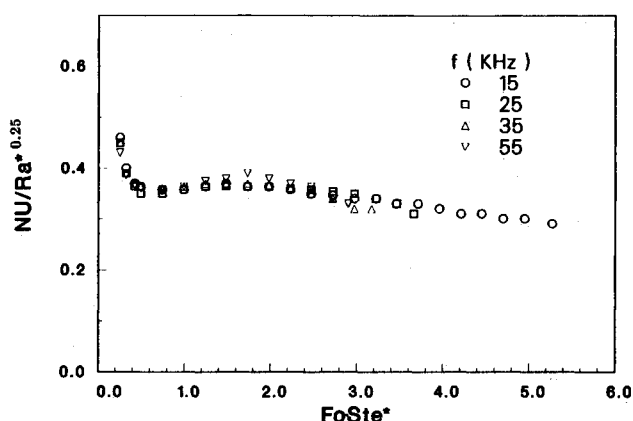


Fig. 6 Dimensionless heat transfer variations on heater surface at various ultrasonic frequencies, $Ra^* = 1.02 \times 10^9$.

melting, whereas the trend is reversed later ($Fo \cdot Ste^* > 0.6$). The reason is that in the early stage of melting the ultrasound causes the solid PCM to be detached a little bit from the test cell, resulting in a gap between the solid PCM and the surrounding enclosure walls, and the molten liquid close to the heater flows to fill the gap. However, once the gap gets filled with liquid PCM, the convective heat transfer begins to increase, due to the ultrasonic vibrations. An interesting feature of these results is that although the magnitude of augmentation in the convection heat transfer is appreciable, the total melting time is significantly affected by the ultrasonic vibrations. This suggests that additional factors exist to enhance the melting process besides the increased convective heat transfer due to the ultrasonic vibrations.

In order to investigate the effect of ultrasonic frequency on the convective heat transfer from the heating plate, several different frequencies (15, 25, 35, and 55 KHz) were applied to the PCM at a constant heat flux of $10.92 \times 10^3 \text{ W/m}^2$. The results are presented in Fig. 6. The frequency of ultrasonic vibrations does not have a significant effect on the convective heat transfer. However, the overall melting process was significantly affected by the frequency of vibrations; that is, as the frequency increases the total melting time decreases. From this observation, it is concluded that although a complete melting process is significantly affected by the ultrasonic waves and the frequency, the enhancement is not only due to the increase of heat transfer from the heater surface.

Melting Characteristics and Solid-Liquid Interface Shape

As previously described, the overall melting phenomena was significantly affected by the applied ultrasonic vibrations. In Table 3, the total melting time was measured and tabulated

for different heat powers. As shown, the ultrasonic vibrations at the frequency of 50 KHz enhanced the overall melting process as much as 2.0–2.7 times greater than the natural melting case. However, since the ultrasonic vibrators consumed electric power of about 60 W, a simple energy balance was considered in order to see actual enhancement by the ultrasound. For this purpose, an ideal melting time of the 5476 cm³ solid paraffin was calculated, where the ideal condition refers to complete insulation of the melting system. The ideal melting time at different power levels are also presented in Table 3. For instance, the ideal time of natural melting at the heat flux of $8.21 \times 10^3 \text{ W/m}^2$ (or 190 W) was calculated at 134 min. Comparing this to the actual melting time of 320 min, the melting efficiency is just 42%. In other words, only 80 W out of 190 W was directly consumed to melt the solid PCM. When ultrasound of 50 KHz was applied, the actual melting time was significantly reduced to 140 min, as shown in Table 3. If the electric power of the transducers (60 W) along with the heater power was completely transmitted to the PCM, the ideal melting time for this case would be 101 min. The melting efficiency with ultrasound becomes 72%, resulting in the 1.7-folds actual enhancement comparing to the natural melting process. However, this enhancement was not solely resulted from the direct input of the transducers' electric power, because the portion of this power to the applied total power was only 24%. Consequently, the ultrasonic waves assisted the input power from the heater to be used more efficiently in the melting phenomena.

The melting phenomena was also significantly affected by the applied ultrasonic frequency, as mentioned in the previous section. The total dimensionless melting time $Fo_f \cdot Ste^*$ is plotted with the ultrasonic frequencies for the heat flux of $10.92 \times 10^3 \text{ W/m}^2$ in Fig. 7. It is noted that, as the frequency increases, the melting process is enhanced until the ultrasonic frequency reaches its optimum value. A correlating equation of dimensionless melting time with frequency for the test conditions used in this study is

$$Fo_f \cdot Ste^* = \frac{12.5}{f(f)} \quad (4)$$

Such enhancement in the melting process has resulted from several effects of ultrasonic waves. Larson and London¹² reported several ultrasonic effects, namely, agitation, acoustic streaming, and cavitation, that increased the heat transfer coefficient for the natural convection and the forced convection at low Reynolds numbers. However, no information of these effects upon the melting phenomena is currently available. In order to investigate the agitation effect on the melting process, another experiment was conducted using a small mechanical stirrer, as described in the previous section of the experimental apparatus. The results of two different cases are presented in Fig. 8. Mechanical stirring was applied at 30 min and 90 min, respectively, after the heat power was applied to the PCM. As shown, both cases of mechanical stirring have a convection heat transfer coefficient on the heater surface approximately 1.5 times greater than the ultrasonic application case. However, the melting process with the ultrasonic vibrations is much faster ($Fo_f \cdot Ste^* = 2.9$) compared to the mechanical stirring case ($Fo_f \cdot Ste^* = 3.8$). From this result, it is concluded that even though the ultrasonic agitation effect might contribute to the enhancement in the melting process to some degree, it is not a sole factor of the enhanced melting process. Also, the cavitation effect by the ultrasound waves results in the augmentation of the melting process. More frequent generation of gas bubbles from the solid-liquid interface was observed during a complete melting process with ultrasonic application. Larson and London¹² stated that, in the case of natural convection heat transfer in liquids, the ultrasonic vibrations could induce the rapid formation and collapse of bubbles, called cavitation, resulting in increased heat transfer. A similar phenomenon can take place in the melting

Table 3 Comparison of melting performance with and without ultrasound

Power, W	Without ultrasound			With ultrasound		
	Ideal melting time, min	Actual melting time, min	η	Ideal melting time, min	Actual melting time, min	η
118	216	520	0.41	143	190	0.75
190	134	320	0.42	102	140	0.73
252	101	230	0.44	82	115	0.71

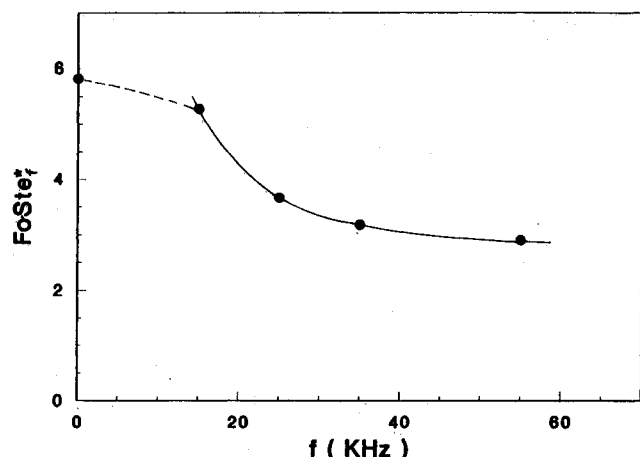
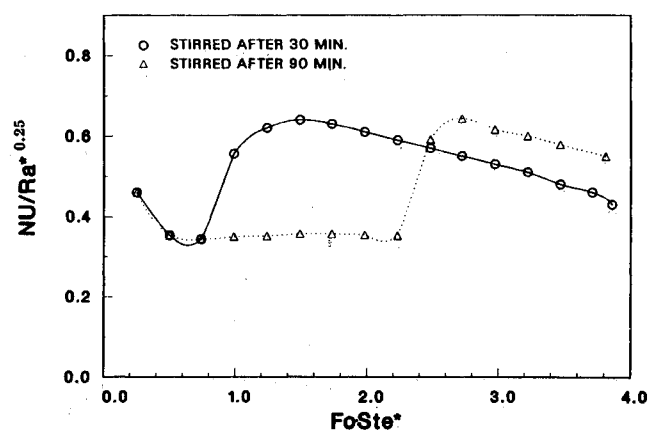
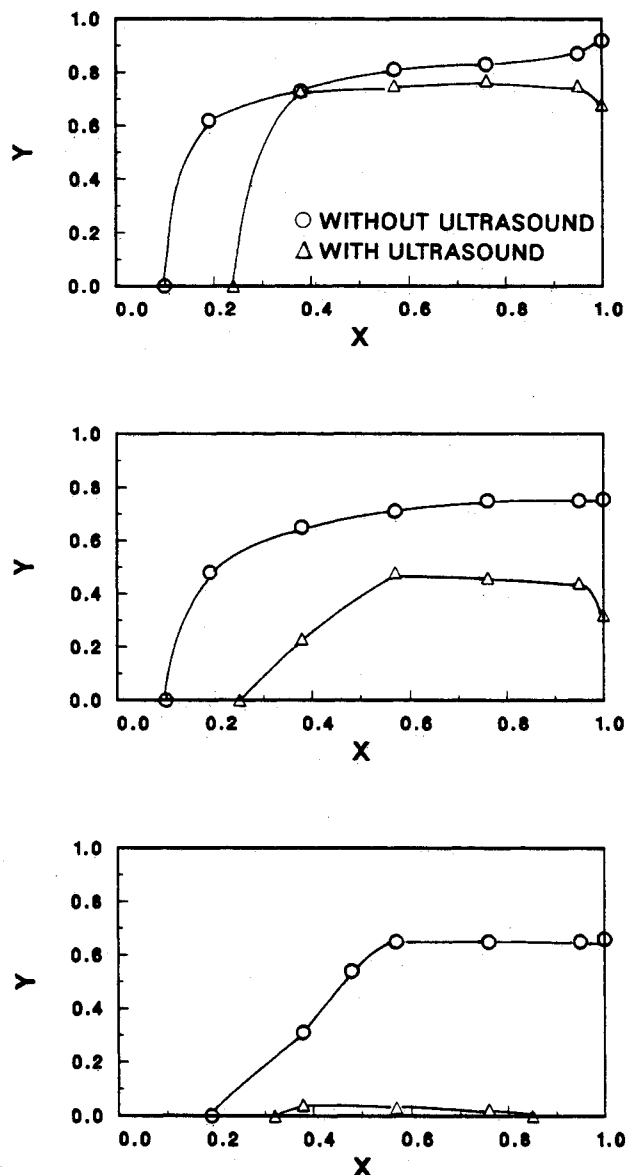


Fig. 7 Variation of dimensionless melting time with ultrasonic frequency.

Fig. 8 Dimensionless heat transfer variations on heater surface for mechanical stirring, $Ra^* = 1.02 \times 10^9$.

process. The applied ultrasonic waves can amplitude the cavitation threshold pressure—the sound pressure amplitude necessary to produce cavitation—around the crevices on the solid-liquid interface. (Several investigators^{17,18} have studied the cavitation threshold pressure for tap water at different frequencies of ultrasonic vibrations.) In addition, the shattering of the solid PCM by the ultrasonic vibrations along the solid-liquid interface appears to be another pronounced effect for the enhanced melting process. During the microscopic shaking of the solid PCM, the bonding force of the solid PCM may become unstable, or microscopic braking-up of the solid, especially in the interface, can occur. In this paper, however, the detailed investigation of these ultrasonic effects upon the melting process has not been attempted. Obviously, the combined effects of ultrasonic waves attribute to the enhancement in the melting process.

From the measurement of the melting depth of PCM, the solid-liquid interface shape was experimentally determined. The interface shapes for $Ra^* = 0.77 \times 10^9$ are presented in Fig. 9 in sequence of dimensionless time $Fo \cdot Ste^*$, where the interface shape was viewed in the x - y plane. A comparison

Fig. 9 Solid-liquid interface shapes in sequence of dimensionless time, $f = 50$ KHz: a) $Fo Ste^* = 1.5$, b) $Fo Ste^* = 2.0$, and c) $Fo Ste^* = 2.5$.

of melting shape under ultrasonic influence for the natural melting case is also presented. The melting shapes are apparently different between the two cases. With the ultrasonic waves, the PCM was melted from the sides both close to and far from the heater surface, for natural melting, the PCM was melted gradually from one side close to the heater. Through a test, it was observed that melting took place not only from the front and rear portions of the PCM but also from the side portions, that is, through all surrounding surfaces of the PCM. This is due to the detachment of solid PCM from the enclosure walls by the ultrasonic vibrations, and, in turn, filling of liquid PCM through the gap.

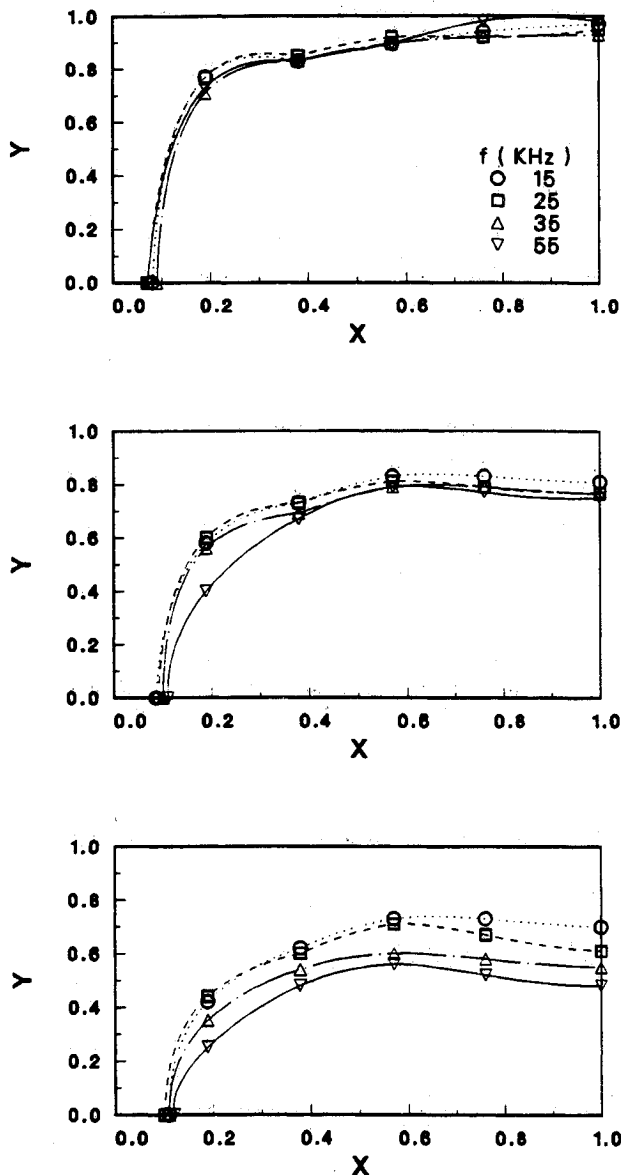


Fig. 10 Solid-liquid interface shapes in sequence of dimensionless time at various frequencies, $Ra^* = 1.02 \times 10^9$: a) $Fo Ste^* = 1.0$, b) $Fo Ste^* = 2.0$, and c) $Fo Ste^* = 2.5$.

The ultrasonic frequency effect on the melting shape is presented in Fig. 10, where four different frequencies were tested at the constant flux. In the early stage of melting, i.e., $Fo \cdot Ste^* < 1.0$, the solid-liquid interface shape was not affected much by the frequency, but later it was significantly influenced. At a higher frequency of ultrasonic waves, the rear portion of PCM had melted more than the middle portion, resulting in augmentation of the melting process. When the melting shape for the low frequency ultrasonic case ($f = 15$ KHz) is compared with the natural melting case shown in Fig. 9, it is noted that no evident difference exists in the melting process. Since the electric power to drive the ultrasonic vibrators was almost constant for all different frequencies, it is concluded that the application of a higher frequency, in the range tested in this study, produces a more efficient melting process.

Temperature Distributions in the PCM

Typical dimensionless temperature distributions in the PCM during a complete melting process at $Ra^* = 0.77 \times 10^9$ are presented in Fig. 11, where the temperatures were measured in three dimensions. Unlike the natural melting case,⁴ the quantitative trend of the temperature distribution is different

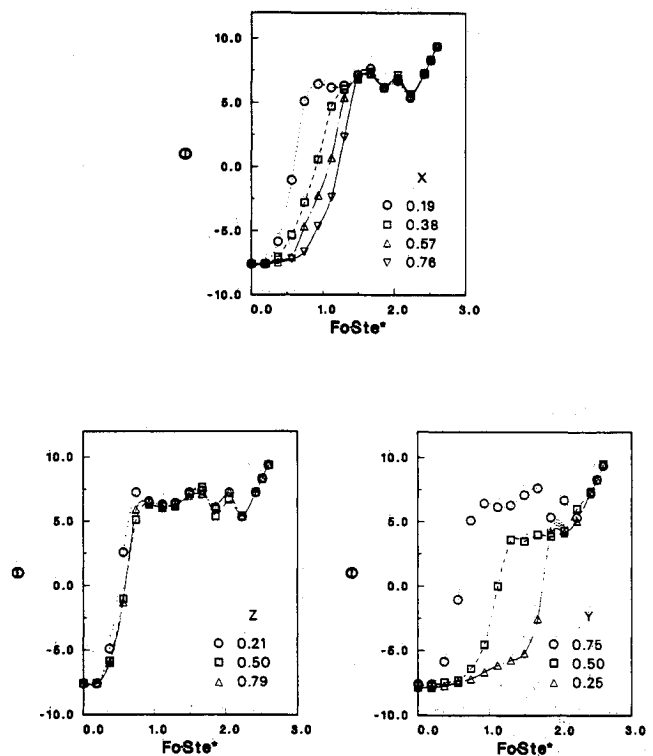


Fig. 11 Dimensionless temperature variations with dimensionless time at various locations: a) $Y = 0.75$ and $Z = 0.5$, b) $X = 0.19$ and $Y = 0.75$, and c) $X = 0.19$ and $Z = 0.5$

for each modified Rayleigh number. As mentioned in the section on heat transfer, the characteristics of the convection heat transfer from the heater could not be generalized in terms of the dimensionless parameters, due to the ultrasonic vibrations. Similarly, the PCM temperature distribution could not be generalized with respect to the modified Rayleigh numbers. From Fig. 11, however, some interesting features of the ultrasonic effect on the PCM temperature field can be observed. Firstly, the liquid temperatures in the top portion of the tank, i.e., $Y = 0.75$, have large fluctuations with time during the melting process, whereas no fluctuations are observed in the lower portion ($Y = 0.5$ or 0.25). Secondly, the temperature distribution in the z -direction is uniform, so the thermal behavior during the melting process can be considered as a two-dimensional problem. Thirdly, the temperatures at various locations in the molten liquid are uniform when the PCM is completely melted, i.e., at $Fo \cdot Ste^* > 2.3$. However, for the natural melting case at the same experimental condition, a thermal stratification with about 6°C difference existed in various locations of the liquid PCM. Whenever natural convection fields in the liquid PCM are induced, due to the associated density gradients in a strong gravitational field, the presence of such a thermal stratification is normal. With the ultrasonic vibrations, the uniformity of liquid temperature in all directions x , y , and z is observed.

Conclusions

The enhancement in the melting process with ultrasonic vibrations in the frequency range of 15–55 KHz was experimentally investigated. The interesting ultrasonic effects upon the melting phenomena are as follows:

1) When the heat energy is coupled with the ultrasonic vibrations of 50 KHz, the overall melting process in the tested geometry is enhanced as much as 1.6–1.8 times greater than without the ultrasound.

2) The frequency of ultrasonic vibrations has a significant effect on enhancement of the melting process. As the frequency decreases, the level of enhancement decreases. At the frequency of 15 KHz, the ultrasonic effects were the mini-

mum, whereas, at the frequency of 55 KHz, the effects were the maximum in the tested range.

3) The ultrasonic effects, such as agitation and acoustic streaming, enhanced the convection heat transfer at the heater surface, however, the enhancement in melting is not solely resulted from the increased convection heat transfer from the heater.

4) With the ultrasonic vibrations, no thermal stratification exists in the completely melted liquid PCM, whereas the thermal stratification exists in the molten liquid PCM without the ultrasound.

5) The ultrasonic vibrations can be properly used to enhance the melting process even at extreme conditions, for instance, if no natural convection takes place.

Acknowledgments

This work was supported partially by the University of Illinois Research Board and by National Science Foundation (CTS 9003015).

References

- ¹Gau, C., and Viskanta, R., "Melting and Solidification of a Pure Metal on a Vertical Wall," *ASME Journal of Heat Transfer*, Vol. 108, No. 1, 1986, pp. 174–181.
- ²Sparrow, E. M., and Geiger, G. T., "Melting in a Horizontal Tube with the Solid Either Constrained or Free to Fall Under Gravity," *International Journal of Heat and Mass Transfer*, Vol. 29, No. 7, 1986, pp. 1007–1019.
- ³Okada, M., "Melting from a Vertical Plate Between Insulated Top and Bottom Surfaces," *ASME-JSME Thermal Engineering Joint Conf.*, Honolulu, Hawaii, Vol. 1, 1983, pp. 281–288.
- ⁴Hong, J. S., "Experimental Study of Melting Phenomena with and without Influence of Ultrasonic Vibrations," M.S. Thesis, Univ. of Illinois at Chicago, June 1988.
- ⁵Viskanta, R., *Phase-Change Heat Transfer, Solar Heat Storage: Latent Heat Materials, Vol. 1*, edited by G. A. Lane, Uniscience Ed., CRC Press, Boca Raton, FL, 1983.
- ⁶Sparrow, E. M., Patankar, S. V., and Ramadhyani, S., "Analysis of Melting in the Presence of Natural Convection in the Melt Region," *ASME Journal of Heat Transfer*, Vol. 99, No. 4, 1977, pp. 520–526.
- ⁷Ho, C.-J., and Viskanta, R., "Heat Transfer During Melting from an Isothermal Vertical Wall," *ASME Journal of Heat Transfer*, Vol. 106, No. 1, 1984, pp. 12–19.
- ⁸Gadgil, A., and Gobin, D., "Analysis of Two-Dimensional Melting in Rectangular Enclosures in Presence of Convection," *ASME Journal of Heat Transfer*, Vol. 106, No. 1, 1984, pp. 20–26.
- ⁹Hendricks, R. C., Simoneau, R., and Dunning, J. W., Jr., "Heat Transfer in Space Power and Propulsion Systems," *Mechanical Engineering*, No. 2, 1986, pp. 41–52.
- ¹⁰Boucher, R. M. G., "Ultrasonics Boosts Heatless Drying," *Chemical Engineering*, No. 19, 1959, pp. 151–154.
- ¹¹Lemlich, R., "Effect of Vibration on Natural Convection Heat Transfer," *Industrial and Engineering Chemistry*, Vol. 47, June 1955, pp. 1175–1180.
- ¹²Larson, M. B., and London, A. L., "A Study of the Effects of Ultrasonic Vibrations on Convective Heat Transfer to Liquids," *ASME*, 62-HT-44, Aug. 1962.
- ¹³Raben, I., "The Use of Acoustic Vibrations to Improve Heat Transfer," *Proceedings of the 1961 Heat Transfer and Fluid Mechanics Inst.*, Stanford Univ. Press, Stanford, CA, 1961.
- ¹⁴Wong, S. W., and Chon, W. Y., "Effects of Ultrasonic Vibration Heat Transfer to Liquids by Natural Convection and by Boiling," *AIChE*, Vol. 15, No. 2, 1969, pp. 281–288.
- ¹⁵Park, K.-A., and Bergles, A. E., "Ultrasonic Enhancement of Saturated and Subcooled Pool Boiling," *International Journal of Heat and Mass Transfer*, Vol. 31, No. 3, 1988, pp. 664–667.
- ¹⁶Fairbanks, H., "Influence of Ultrasound upon Heat Transfer Systems," *Ultrasonics Symposium*, Inst. of Electrical and Electronics Engineers, 1979, pp. 384–387.
- ¹⁷Strasberg, M., "Onset of Ultrasonic Cavitation in Tap Water," *Journal of the Acoustical Society of America*, Vol. 31, No. 2, 1959, pp. 163–176.
- ¹⁸Connolly, W., and Fox, F. E., "Ultrasonic Cavitation Thresholds in Water," *Journal of the Acoustical Society of America*, Vol. 26, No. 5, 1954, pp. 843–848.